Lactic Acid Upregulates VEGF Expression in Macrophages and Facilitates Choroidal Neovascularization

Juha Song,[1,2] Kihwang Lee,[3] Sung Wook Park,[4] Hyewon Chung,[1] Daun Jung,[1] Yi Rang Na,[1] Hailian Quan,[1] Chang Sik Cho,[4] Jeong-Hwan Che,[5] Jeong Hun Kim,[4] Jae-Hak Park,[2] and Seung Hyeok Seok[1]

[1]Department of Microbiology and Immunology, Institute of Endemic Disease, Seoul National University College of Medicine, Chongno-gu, Seoul, South Korea
[2]Department of Laboratory Animal Medicine, College of Veterinary Medicine, Seoul National University, Gwanak-gu, Seoul, South Korea
[3]Department of Ophthalmology, Ajou University School of Medicine, Suwon-si, South Korea
[4]FARB Laboratory, Biomedical Research Institute, Seoul National University Hospital, Seoul, South Korea
[5]Biomedical Research Institute, Seoul National University Hospital, Chongno-gu, Seoul, South Korea

Correspondence: Jae-Hak Park, Department of Laboratory Animals, College of Veterinary Medicine, Seoul National University, 1, Gwanak-ro, Gwanak-gu, Seoul 08826, South Korea;
pjhak@snu.ac.kr.
Seung Hyeok Seok, Department of Microbiology and Immunology, Seoul National University College of Medicine, 103, Daehak-ro, Jongno-gu, Seoul 03080, South Korea;
lamseok@snu.ac.kr.

JS and KL contributed equally to the work presented here and should therefore be regarded as equivalent authors.

Submitted: January 18, 2018
Accepted: June 13, 2018

Citation: Song J, Lee K, Park SW, et al. Lactic acid upregulates VEGF expression in macrophages and facilitates choroidal neovascularization. *Invest Ophthalmol Vis Sci*. 2018;59:3747–3754. https://doi.org/10.1167/iovs.18-23892

Purpose. Lactic acid, the end product of glycolysis, has emerged as an immune-modulating metabolite in various diseases. In this study, we aimed to examine whether lactic acid contributes to the disease pathogenesis of choroidal neovascularization (CNV) and to investigate the role of macrophages in CNV pathogenesis.

Methods. CNV was induced by laser photocoagulation in C57BL/6J mice. Lactic acid concentration was measured in the RPE-choroid region. Macrophage infiltration and VEGF were quantified by flow cytometry. VEGF-positive areas and CNV lesions were measured by flat-mount immunofluorescence staining. To inhibit lactic acid uptake in vivo, alpha-cyano-4-hydroxycinnamic acid (α-CHC), a monocarboxylate transporter (MCT) blocker, was injected intravitreally 1 day after laser. VEGF productions were measured in ARPE-19, THP-1 cells, and human umbilical vein endothelial cells (HUVECs) by quantitative PCR and ELISA. Angiogenic activity of lactic acid–treated macrophages was assessed by HUVEC tube formation assay.

Results. Lactic acid was significantly increased in the RPE-choroid region of CNV-induced mice. Lactic acid upregulated *VEGFA* mRNA and VEGF protein expressions in THP-1 macrophages, but did not in ARPE-19 or HUVECs. THP-1 macrophages treated with lactic acid increased the angiogenesis of endothelial cells independent of MCT activity. Intravitreal injection of α-CHC substantially reduced the VEGF-positive area that colocalized with F4/80-positive macrophages. CNV lesions were also significantly reduced following α-CHC injection compared with vehicle-injected controls.

Conclusions. To our knowledge, these results show for the first time the role of lactic acid in facilitating neovascularization through macrophage-induced angiogenesis. We suggest that targeting macrophage metabolism can be a promising strategy for CNV treatment.

Keywords: lactic acid, choroidal neovascularization, VEGF, macrophages, α-CHC

Choroidal neovascularization (CNV), a wet form of AMD, is a worldwide leading cause of visual impairment and legal blindness in people older than 50.[1] Newly formed blood vessels extend anteriorly through breaks in Bruch's membrane and invade the subretinal space, resulting in hemorrhage, fluid exudation, and, eventually, photoreceptor degeneration.[2] Experimental data suggest that CNV results from responses of the RPE to heterogeneous stressors, including aging, smoking, or genetic predisposition, creating microenvironments that promote abnormal neovascularization.[3] There have been many efforts to discover reliable indicators of CNV development. Of note, recent findings suggest that assessing for altered metabolic states could be a comprehensive means for identifying CNV progression.[4–8]

Lactic acid, the end product of metabolic glycolysis, is an active metabolite that accumulates at sites of inflammation and modulates cell signaling.[9–11] Considered to be a metabolic hallmark of pathological conditions such as chronic inflammatory diseases and cancer, lactic acid is known to induce functional reprogramming in various cells including macrophages.[11–14] With regard to the eye, RPE, primarily relies on oxidative phosphorylation (OXPHOS) to sustain crucial cellular functions in maintaining metabolic homeostasis by transporting excess lactate from the metabolically active retina to the choroidal vessel.[15–17] During CNV pathogenesis, however, RPE is perturbed by chronic inflammation and oxidative stress, resulting in a metabolic switch from OXPHOS to glycolysis and irreversible dysfunction.[16,18,19] These processes are assumed to induce lactic acid accumulation in subretinal space; however, there is sparse research evaluating the metabolic influence of lactic acid on CNV.

In this study, we sought to demonstrate lactic acid accumulation in CNV disease and identify its impact on surrounding cells, including RPE, infiltrated macrophages, and choroidal endothelial cells, and finally on neovascularization. In

Copyright 2018 The Authors

This work is licensed under a Creative Commons Attribution-NonCommercial-NoDerivatives 4.0 International License.

Downloaded from iovs.arvojournals.org on 04/13/2021

particular, we focused on the effect of lactic acid on VEGF expression, which is strongly implicated in CNV development. Here, we demonstrate that lactic acid was significantly increased in laser-induced CNV mice. Through in vitro and in vivo studies, lactic acid was found to serve as a proangiogenic agent by increasing VEGF content in macrophages, and no other surrounding cells. This was effectively inhibited via blockade of lactic acid uptake by treatment of monocarboxylate transporter blocker, α-cyanohydroxycinnamic acid (α-CHC). Finally, α-CHC–injected CNV mice showed significantly reduced neovascular lesions compared with vehicle-treated mice. Thus, blockade of lactic acid signaling in macrophages may have antiangiogenic effects and should be considered for future therapeutic application in CNV.

Materials and Methods

Cell Lines and Reagents

Human APRE-19 cells were obtained from ATCC (Manassas, VA, USA) and cultured in Dulbecco's modified Eagle's medium (DMEM)/F12 media (1:1) supplemented with 10% fetal bovine serum (FBS) (Gibco, Carlsbad, CA, USA), 1% penicillin-streptomycin (Gibco), and 2 mM L-glutamine (Gibco) in a humidified incubator at 37°C and 5% CO_2. For ARPE-19 monolayer culture, cells were seeded in 24-well tissue culture plates (1.5×10^5 cells per well; Corning, Corning, NY, USA) and maintained in DMEM/F12 media with reduced serum (1% FBS). Confluent monolayer cultures with transepithelial resistance (TER) greater than 40 Ωcm^2 were used for experiments. Human umbilical vein endothelial cells (HUVECs; Lonza Ltd., Basel, Switzerland) were purchased and cultured in endothelial growth medium-2 (EGM-2) (Lonza). The human acute monocytic leukemia THP-1 cell line was maintained in RPMI media containing 10% FBS (Gibco). Differentiation of THP-1 cells into macrophages was performed by incubation with 15 ng/mL phorbol 12-myristate 13-acetate (PMA) (Sigma-Aldrich Corp., St. Louis, MO, USA) for 2 days at 37°C with 5% CO_2.

Cell Treatments

Confluent ARPE-19 monolayer cells maintained in 24-well plates were incubated with 10 mM L(+)-Lactic acid (Sigma-Aldrich Corp.), in the presence or absence of 3 mM monocarboxylate transporter blocker α-CHC (Sigma-Aldrich Corp.) for the designated time periods. HUVECs were seeded in 24-well plates at a density of 1×10^5/well. When the cells reached 60% to 70% confluence, cells were exposed to 10 mM L(+)-lactic acid with or without 3 mM α-CHC. THP-1 cells plated in 24-well plates at a density of 3×10^5/well and differentiated into the macrophages by PMA treatment were incubated with 20 mM L(+)-Lactic acid with or without 3 mM α-CHC.

Animals

Female wild-type C57BL/6J mice (Samtako Co., Gyeonggi, Korea) between 7 and 8 weeks of age were used in this study. The study protocol was approved by the Seoul National University Animal Care and Use Committee (Approval No. SNU-160114-1). All animal experiments were conducted in accordance with the guidelines of the ARVO Statement for the Use of Animals in Ophthalmic and Vision Research.

Metabolite Extraction

RPE-choroid tissues were isolated from mice and metabolite extraction was performed according to a previously described method with minor modifications.[20] Briefly, freshly isolated tissues were homogenized in 100 μL 1M perchloric acid (PCA) solution and incubated on ice for 30 minutes. After centrifugation at 15,871*g* for 15 minutes, 2M KOH (0.25 μL per 1 μL PCA) was added to the supernatant to neutralize the PCA. After centrifugation at 15,871*g* for 15 minutes again, the resulting supernatant was subsequently used for lactate measurement.

Lactate Measurement

Lactate concentration was measured using a Lactate Colorimetric/Fluorometric Assay Kit (BioVision, Milpitas, CA, USA) as per the manufacturer's protocol.

Enzyme-Linked Immunosorbent Assay

Cells were treated with lactic acid for 24 hours. The media was collected, centrifuged at 587*g* for 5 minutes to remove particulates and stored at −80°C until ELISA was performed.

Retina and RPE-choroid tissues were isolated from naïve or CNV (3 days after laser) mice, and homogenized in ice-cold RIPA lysis buffer (Thermo Scientific, Rockford, IL, USA) containing 1% protease inhibitor cocktail and 1% phosphatase cocktail (GenDEPOT, Katy, TX, USA). After centrifugation at 15,871*g* for 15 minutes, the supernatant was used for ELISA assay. The secretion of VEGF was measured by use of the ELISA Duoset system (R&D Systems, Minneapolis, MN, USA) according to the manufacturer's instructions.

RNA Isolation and Real-Time RT-PCR

Total RNA was extracted from cells with Trizol (Invitrogen, Carlsbad, CA, USA) following the manufacturer's instructions. RNA concentration/quality was assessed by NanoDrop spectrophotometer (NanoDrop Technology, Wilmington, DE, USA). Equal amounts of RNA were reverse transcribed into cDNA with Reverse Transcription kits (Enzynomics, Daejeon, Korea) and gene expression was determined by quantitative real-time PCR using SYBR Green PCR Master Mix (Applied Biosystems, Foster City, CA, USA) on an ABI PRISM 7900 (Applied Biosystems). The relative mRNA expressions of each sample were normalized by *β-actin* and RPL37A and Student's unpaired *t*-test was used for statistical analysis. Sequences of primers used for amplifications were as follows: *β-actin*: FP, 5′-ATTGCCGACAGGATGCAGAA-3′; RP, 5′-GCTGATCCACATCTGCTGGAA-3′. *RPL37A:* FP, 5′-ATTGAAATCAGCCAGCACGC-3′; RP, 5′-AGGAACCACAGTGCCAGATCC-3′. *VEGFA*: FP, 5′-ATTGAAATCAGCCAGCACGC-3′; RP, 5′-AGGAACCACAGTGCCAGATCC-3′.

Laser-Induced CNV in Mice

Female C57BL/6J mice, aged 7 to 8 weeks, were anesthetized with an intraperitoneal injection of ketamine-xylazine (10 mg/kg), and the pupils were dilated with 1% tropicamide (Alcon Laboratories Inc., Fort Worth, TX, USA). Treatment with 831-nm 106 diode laser photocoagulation (75 μm spot size, 0.1-second duration, 120 mW) was delivered to each 3, 6, 9, and 12 o'clock position of two disc-diameters from the optic disc by using an indirect head set delivery system of a photocoagulator (OcuLight; Iridex, Mountain View, CA, USA) and a handheld +78-diopter lens. The bubbling or pop sensing with laser photocoagulation was considered to be successful rupture of Bruch's membrane. These cases of successful rupture were included in this study. To evaluate the antiangiogenic effect of blocking lactate uptake in macrophages, we injected 2 μL 3 mM α-CHC dissolved in PBS intravitreally

Investigative Ophthalmology & Visual Science

Downloaded from iovs.arvojournals.org on 04/13/2021

1 day after laser coagulation, when macrophages begin to infiltrate the burned area.

Immunohistochemistry

THP-1 cells differentiated with 15 ng/mL of PMA for 48 hours were treated with lactic acid for 18 hours, and fixed for 15 minutes in 4% paraformaldehyde. After blocked in 5% FBS in PBS containing 0.3% Triton X-100 for 1 hour, cells were incubated at 4°C overnight with the following primary antibodies: FITC-conjugated CD68 (KP1; Santa Cruz Biotechnology, Inc., Santa Cruz, CA, USA) and APC-conjugated anti-mouse VEGF (C-1, Santa Cruz Biotechnology, Inc.). The cells were rinsed and washed three times with PBS. Finally, to stain nuclei, cells were treated for 15 minutes with 3 μM of the nuclear stain 4′,6-diamidino-2-phenylindole (DAPI). The stained cells were observed under a Olympus FV1000 Confocal Scanning Scope (Olympus, Tokyo, Japan). The VEGF intensity was measured using ImageJ software (http://imagej.nih.gov/ij/; provided in the public domain by the National Institutes of Health, Bethesda, MD, USA).

Three days after laser photocoagulation, eyes were enucleated from mice and fixed for 1 hour in 4% paraformaldehyde. After removal of the retina, RPE-choroid tissues were incubated with rat anti-mouse F4/80 (Bio-Rad, Richmond, CA, USA) and APC-conjugated anti-mouse VEGF (C-1; Santa Cruz Biotechnology, Inc.) at 4°C overnight. The flat-mount was washed with PBS 10 times for 10 minutes on an orbital shaker at room temperature and then incubated with Alexa-Fluor 488-labeled goat anti-rat IgG (Molecular Probes, Eugene, OR, USA) for 1 hour on an orbital shaker at room temperature. The stained tissues were examined under an Olympus FV1000 Confocal Scanning Scope. The areas of infiltrated macrophage and secreted VEGF were measured using ImageJ software.

Histology

Fixed globes after laser induction were embedded in paraffin and processed for standard hematoxylin and eosin (H&E) staining to assess standard morphology. Stained sections were digitized using a light microscopy (Labophot; Nikon, Tokyo, Japan).

CNV Quantification

For the assessment of CNV, RPE-choroid tissues isolated from the eyes 7 days after laser were stained with Alexa-Fluor 594-conjugated isolectin B4 (Molecular Probes) to visualize CNV. Images acquired with Olympus FV1000 Confocal Scanning Scope were processed in IMARIS imaging software (Bitplane, Zurich, Switzerland) to quantify IB4-positive CNV volume.

Flow Cytometry

THP-1 cells differentiated with 15 ng/mL of PMA for 48 hours were treated with lactic acid for 18 hours. After fixed and permeabilized, cells were stained with APC-conjugated anti-mouse VEGF (C-1; Santa Cruz Biotechnology, Inc.). Labeled cells were analyzed using LSR-II cytometer (BD Biosciences, San Jose, CA, USA), and the data were analyzed using FlowJo Software (version 7.6.2; Ashland, OR, USA).

Laser-treated eyes were enucleated microsurgically 1, 3, 7, 14, and 21 days after laser treatment. After removing the anterior segment and vitreous humor, the posterior segment containing the retina and RPE-choroid was subsequently dissociated enzymatically for 1 hour with 1 mg/mL type I collagenase (Sigma-Aldrich Corp.) in the presence of 50 units/mL DNase I (Sigma-Aldrich Corp.). Single-cell suspension in PBS was washed by centrifugation at 685*g* for 5 minutes, and then cell pellets were suspended with 200 μL FACS buffer containing 1% BSA and 0.1% sodium azide. For surface staining, the following antibodies were used: Q655-conjugated anti-mouse CD45 (clone: 30-F11; eBioscience, San Diego, CA, USA), PE-conjugated anti-mouse F4/80 (clone: BM8; eBioscience), APC eFluor 780-conjugated anti-mouse CD11b (clone: M1/70; eBioscience), V450-conjugated anti-mouse Gr-1 (clone: RB6-8C5; eBioscience), FITC-conjugated anti-rat CD206 (clone: MR5D3; AbD Serotec, Raleigh, NC, USA). To detect intracellular cytokines, cells were fixed and permeabilized in BD Perm/Wash buffer (BD Pharmingen, San Diego, CA, USA) before incubation with the following antibodies: APC-conjugated anti-mouse VEGF (C-1, Santa Cruz Biotechnology, Inc.). Labeled cells were analyzed using LSR-II cytometer (BD Biosciences), and the data were analyzed using FlowJo Software (version 7.6.2).

Tube Formation Assay

Growth factor-reduced Matrigel (Corning) was thawed at 4°C overnight. Each well of a prechilled 24-well plate was coated with 100 μL Matrigel and incubated at 37°C for 40 minutes. HUVECs (3×10^4 cells) were suspended in 100 μL EGM-2 media and seeded with 400 μL macrophage conditioned media. After 12 hours of incubation at 37°C with 5% CO2, endothelial cell tube formation was visualized with Calcein AM (Corning) and then imaged using a Leica CTR6000 fluorescence microscope (Wetzlar, Germany). The number of capillary-like structures was quantified by manual counting of low-power fields (×10). Five independent fields were assessed for each well, and the average number of branches per field (magnification, ×10) was determined.

Statistical Analysis

All results are expressed as the means ± SEM. Statistical significances between groups were evaluated with the Student's unpaired *t*-test (two-tailed). $P < 0.05$ was considered to be statistically significant.

Results

Elevated Lactic Acid Levels in RPE-Choroidal Region of CNV

CNV was induced by laser burn and RPE-choroid tissue was isolated for metabolite extraction (Fig. 1A). CNV lesions at day 1 were stained with H&E and found to have broken RPE layers and Bruch's membrane rupture compared with unlasered controls (Figs. 1B, 1C). To evaluate the lactic acid concentration in CNV, metabolites extracted from RPE-choroid tissues were analyzed by ELISA. As shown in Figure 1D, lactic acid levels in RPE-choroid tissues were significantly increased compared with unlasered controls.

Lactic Acid Induces Macrophages to Become Proangiogenic

During CNV development, crosstalk of RPE with immune cells and the vascular system has been reported to be a key event in CNV development.[3] Increased production of VEGFA by cells participating in these processes has been implicated as the main contributor to abnormal angiogenesis, and has therefore been a therapeutic target for neovascular AMD.[1,21] Considering previous studies on the signal-inducing ability of lactic acid, we wondered whether lactic acid affects VEGF

Investigative Ophthalmology & Visual Science

Downloaded from iovs.arvojournals.org on 04/13/2021

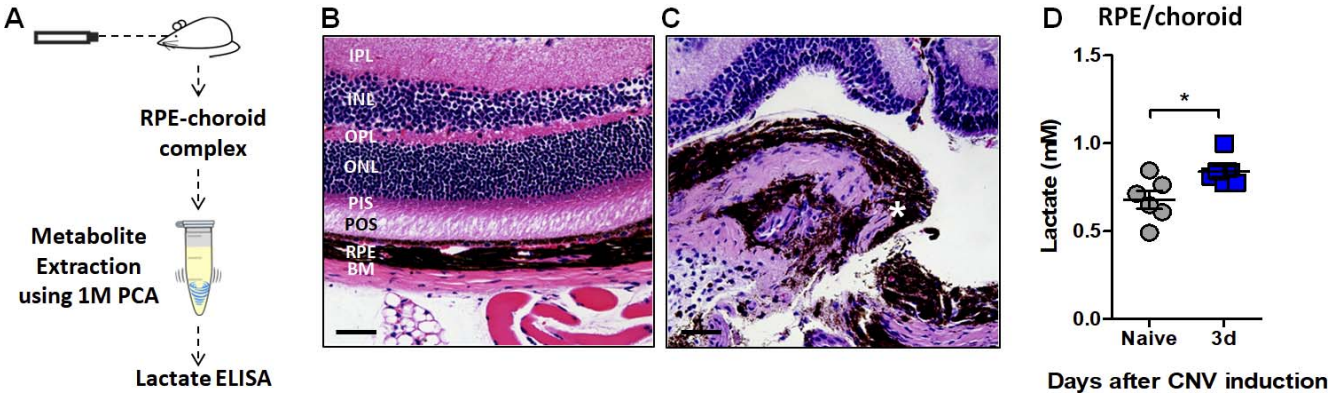

FIGURE 1. Lactic acid is increased in RPE-choroid regions of CNV-induced mice. (**A**) Schematic image describing CNV inducing and lactic acid measurement. (**B**, **C**) Representative retinal histology before injury (**B**) and 1 day after injury (**C**). H&E stained. $n = 6$. Broken RPE is marked by the *asterisk*. IPL, inner plexiform layer; INL, inner nuclear layer; OPL, outer plexiform layer; ONL, outer nuclear layer; PIS, photoreceptor inner segment; POS, photoreceptor outer segment; BM, Bruch's membrane. *Scale bars*: 50 μm. (**D**) Lactate concentrations of RPE-choroid regions measured by a lactate colormetric/fluorometric assay kit. $n = 6$. *Bars* indicate means ± SEM. $^*P < 0.05$.

secretion by cell types in the eye. To directly study the contribution of lactic acid to the VEGF expression of RPE, endothelial cells, and infiltrated macrophages, we conducted in vitro cell line experiments using ARPE-19, HUVEC, and PMA-differentiated THP-1 macrophages. Cells were treated with 20 mM lactic acid. *VEGFA* mRNA and VEGFA protein expression were assessed by real-time RT-PCR and ELISA, respectively. Gene transcript and protein expression for VEGFA in ARPE-19 and HUVECs did not change after lactic acid treatment (Figs. 2A, 2B, Supplementary Fig. S1); however, PMA-differentiated THP-1 macrophages showed significant increase in *VEGFA* mRNA expression and peaked at 12 hours post-stimulation by more than 3-fold (Fig. 2C, Supplementary Fig. S1). Secreted VEGF also significantly increased by approximately five times in THP-1 macrophages incubated with lactic acid for 24 hours, which was reduced by pretreatment of 3 mM monocarboxylate transport blocker, α-CHC (Fig. 2D). This was further confirmed by analyzing VEGF content of THP-1 macrophages after incubation with lactic acid for 18 hours using flow cytometry and immunofluorescence staining technique (Supplementary Fig. S2). Importantly, THP-1 macrophages exposed to media acidified to pH 4.5 with HCl did not show any significant changes in VEGF expression, indicating that VEGF upregulation by lactic acid is not due to the acidification of culture media.

Then, to identify whether lactic acid–stimulated macrophages promote angiogenesis, we performed HUVEC tube formation assay. PMA-differentiated THP-1 macrophages were stimulated with 20 mM lactic acid for 12 hours, and media was then changed. Tube-forming ability of supernatant collected after 24-hour incubation was compared with that of nonstimulated cells and α-CHC–pretreated cells. As shown in Figure 2E, enhanced endothelial tube formation was observed in lactic acid–conditioned media compared with that of nontreated media, whereas supernatant of α-CHC–pretreated lactic acid–stimulated macrophages exhibited clear reduction in the amount of tube formation of HUVECs. A 5-fold increase in number of branches formed by lactic acid–conditioned media was also substantially reduced by α-CHC and lactic acid cotreated conditioned media (Fig. 2F), indicating that macrophages exposed to lactic acid are programmed to be proangiogenic.

Infiltration and VEGF Expression of Macrophages in CNV

To investigate the effect of lactic acid in vivo, we first assessed macrophage infiltration into CNV lesions by flow-cytometric analysis. The number of recruited macrophages ($CD45^+$ $CD11b^+$ $Gr1^-$ $F4/80^+$) increased at 1 day after laser and peaked at 3 days with an increase of more than 10-fold compared with that of nonlasered controls (Figs. 3A, 3B). Intracellular VEGF content per single macrophage cell at day 3 after laser treatment was significantly upregulated compared with that of unlasered controls (Figs. 3C, 3D), providing further evidence of the proangiogenic properties of macrophages.

Inhibitory Effect of α-CHC on Neovascularization

The effect of lactic acid on VEGF expression in macrophages and subsequent aberrant neovascularization was confirmed by intravitreal injection of monocarboxylate transporter blocker α-CHC 1 day after CNV induction. Injection of 2 μL 3-mM α-CHC resulted in significant reduction of VEGFA contents in macrophages at 3 days after laser shot (Figs. 4A, 4B). Flat-mount immunofluorescence staining also showed the significant reduction of VEGF-positive area (383,738 ± 196,716 μm^2) within F4/80-stained macrophage area compared with controls (523,378 ± 165,071 μm^2) (Figs. 4C, 4E), although the area of infiltrated macrophages showed no significant changes (Fig. 4D). The VEGF levels in RPE-choroid tissues at day 3 (2120.5 ± 286.4 VEGF pg/tissue g) and isolectin B4 (IB4)-positive endothelial cells at day 7 (141,472.9 ± 49,186.4 μm^3) after laser burn were both substantially reduced by α-CHC injection (1138.9 ± 109.7 VEGF pg/tissue g and 74,160.6 ± 12,339.5 μm^3, respectively) (Figs. 4D–F), suggesting that modulation of macrophages by blocking lactic acid transport has a promise for CNV therapeutics.

DISCUSSION

This study revealed, for the first time, that the glycolytic end product, lactic acid, increases VEGF production by macrophages to foster CNV development in the eye. We demonstrated several important findings. First, an increase of lactic acid concentration was consistently observed in the RPE-choroid tissues of experimental CNV model. Second, lactic

Investigative Ophthalmology & Visual Science

Downloaded from iovs.arvojournals.org on 04/13/2021

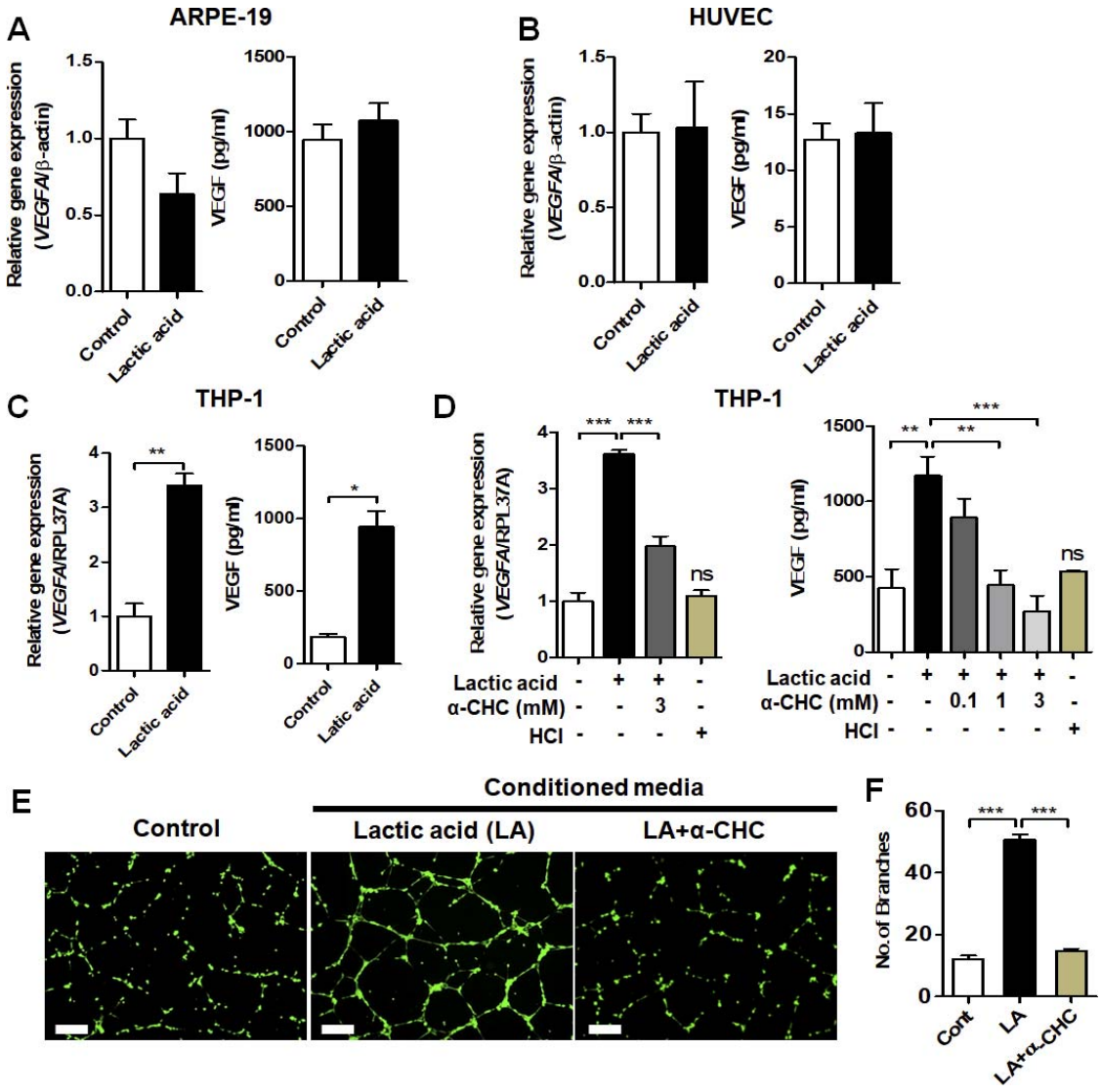

Figure 2. Lactic acid induces VEGF expression in macrophages and facilitates angiogenesis. (**A–C**) Expression analysis by qPCR and ELISA of VEGF in ARPE-19 (**A**), HUVEC (**B**), and PMA-differentiated THP-1 macrophages (**C**) was conducted following incubation with control or 20 mM of lactic acid (LA)-treated medium. (**D**) Expression analysis of VEGF in THP-1 macrophages was conducted following incubation with lactic acid ± MCT blocker α-CHC and acidic pH necessary for the effect of lactic acid. (**E**, **F**) Tube formation assay. HUVECs were seeded onto Matrigel-coated plates with control THP-1 supernatant, lactic acid–stimulated THP-1 supernatant in the presence or absence of α-CHC. Representative images of capillary-like structures stained with Calcein AM are shown (**E**). Total branching point was calculated using ImageJ software (**F**). Data are representative of three independent experiments. *Bars* indicate means ± SEM. $^{*}P < 0.05$, $^{**}P < 0.01$, $^{***}P < 0.001$.

acid–stimulated macrophages substantially enhanced the tube formation of HUVECs, which was diminished by α-CHC pretreatment. Finally, blocking lactic acid transport by intravitreal injection of α-CHC in CNV mice significantly reduced VEGF expression in macrophage-infiltrated areas, total VEGF content in RPE-choroid tissues, and subsequent neovascularization.

Previously, Winkler[22] reported that altered metabolic states by hyperglycemia or hypoxia resulted in human retinal lactate accumulation 3- or 7-fold, respectively. In the case of AMD, pyruvate, lactate, and lactate/pyruvate ratio were substantially increased in urine samples collected from typical AMD patients,[6] suggesting that glycolysis may contribute to age-related microvascular alterations. Our results showing significant increases of lactic acid levels in laser-burned RPE-choroid complexes in mice might give insights in those findings from human AMD patients because we proved that lactic acid is associated with CNV pathogenesis by potentiating macrophage-mediated VEGFA secretion (Fig. 1D). Although it is difficult to know the exact levels of lactate in subretinal space, it is presumed to be significantly elevated due to, at least, the glycolytic shift of damaged RPE-choroid cells. However, the possibility of lactic acid accumulation due to blockade of transport from retina to choroid remains to be elucidated.

This study points to an active role of lactic acid on macrophages during neovascularization. The 20 mM lactic acid significantly upregulated VEGF expression by human THP-1 macrophages, promoting tube formation of HUVECs (Fig. 2). Similarly, Zhu et al.[23] also demonstrated that an increase of retinal lactate by 30 mM in pathological states contributes to retinal VEGF production. It has also been reported that blood and muscle lactate levels can rise as high as 30 mM by extensive exercise.[23,24] Considering that the eye has 10 mM of lactate at normal steady-states and that chronic inflammation

Investigative Ophthalmology & Visual Science

Downloaded from iovs.arvojournals.org on 04/13/2021

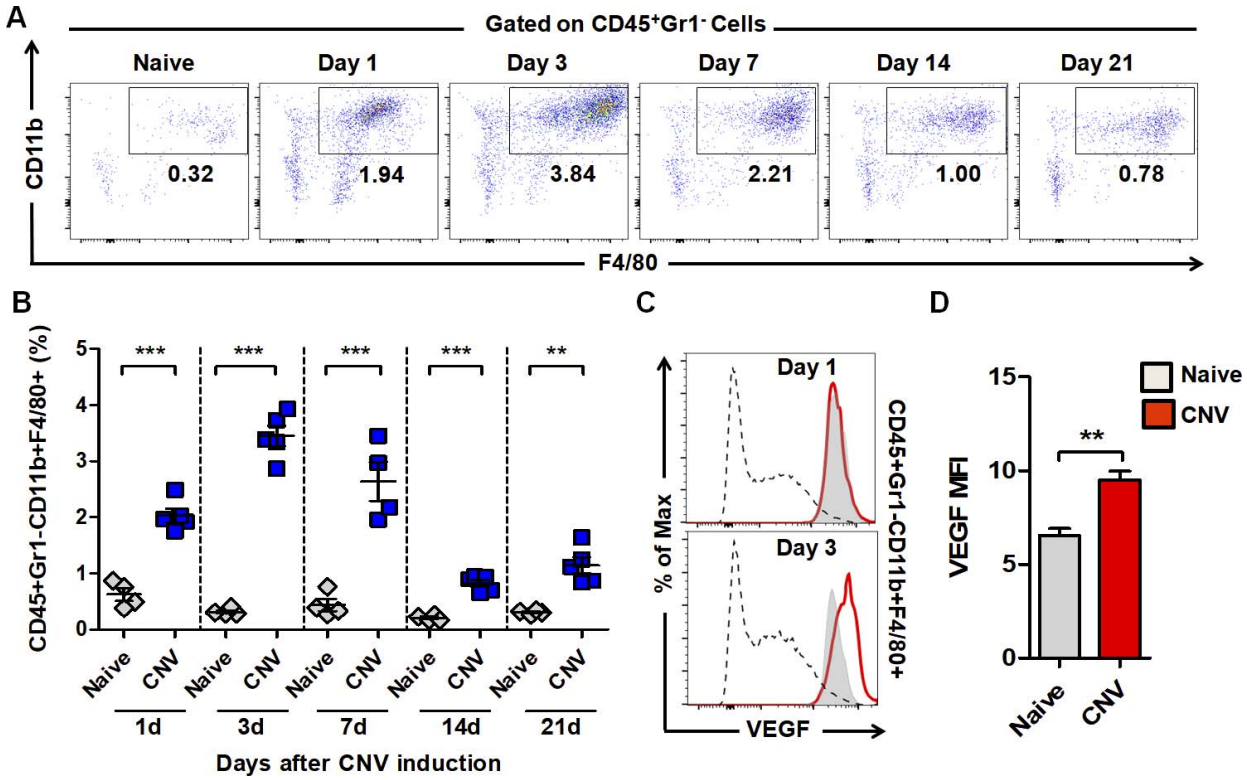

FIGURE 3. Macrophage infiltration and their VEGF secretion are increased in RPE-choroid regions in CNV mice. (**A**, **B**) Posterior eyecups of mice after induction of CNV were enzymatically dissociated and analyzed by flow cytometry for macrophage markers (**A**). The percentages of macrophages infiltrating the eye are shown ($n = 5$ per group) (**B**). (**C**, **D**) VEGF expression by macrophages at 3 days after laser was analyzed by flow cytometry. Representative histograms are shown ($n = 5$ per group) (**C**). Percentage of VEGF MFI was calculated in the indicated populations (**D**). *Bars* indicate means ± SEM. $^{*}P < 0.05$, $^{**}P < 0.01$, $^{***}P < 0.001$.

and hypoxic stress may increase lactate levels, 20 mM of lactate is a feasible concentration that could be expected to be found in CNV pathogenesis.[22,25]

The molecular mechanism of VEGF induction by lactic acid is thought to be related to the activation of pH-sensing G protein–coupled receptor 132 (Gpr132, also known as G2A), which is highly expressed in macrophages.[26–28] In a GPR132-dependent manner, lactate-stimulated macrophages alternatively display an activated (M2) phenotype exhibiting CD206 and Arginase-1.[29] The downstream molecule, hypoxia-inducible factor 1α (HIF1α), which has been reported to be an essential mediator for M2 polarization of tumor-associated macrophages by tumor-derived lactic acid, is also suspected to be involved.[14]

Here, we show that macrophage infiltration significantly increases at the site of neovascular lesions during CNV development (Figs. 3A, 3B). Our data showing elevated VEGF production by these macrophages suggests that macrophages potentiate angiogenic capacity in CNV. This is consistent with previous reports that show that invading macrophages exhibit increased VEGF expression.[30,31] Inhibition of CCR2, therefore, resulted in CNV suppression by reducing macrophage infiltration.[32,33] The proangiogenic role of invading macrophages was also demonstrated by the attenuation of neovascularization after removal of monocytes and macrophages following clodronate liposome injection in CNV mice.[34,35] These experimental results strongly imply the therapeutic potential of macrophage targeting in CNV treatment.

Although the current treatment of AMD with intravitreal anti-VEGF injection offers new hope to thousands of patients with neovascular AMD, there are risks of adverse effects, including severe atrophy of choriocapillaris due to repeated treatment.[36–38] In contrast, targeting macrophages to blunt excessive VEGF upregulation can be a promising strategy in CNV therapy. A previous report showed that inhibition of M2-type macrophage polarization by doxycycline as an alternative therapeutic approach against long-term anti-VEGF treatments, attenuated IL-1β–induced pathological blood vessel growth.[39] Zandi et al.[40] also identified that inhibition of ROCK isoforms, which are associated with M2 shift, can reduce CNV incidence. Of note, our study targets a metabolic pathway to inhibit the proangiogenic activity of macrophages using the monocarboxylate transporter 1 (MCT1) blocker α-CHC, suggesting that this may be an alternative or adjunct therapeutic approach to anti-VEGF treatment (Fig. 4). Alpha-CHC has been used to inhibit lactic acid–induced signals promoting proliferation and migration in MCT1-expressing cells, such as endothelial cells and cancer cells.[14,41,42] For example, daily intraperitoneal injections of α-CHC blocked angiogenesis in LLC tumors subcutaneously implanted in mice. In our study, lactic acid and α-CHC may have direct effects on endothelial cell proliferation and neovascularization in CNV mice. Nevertheless, our experiments performed in CNV mice show a clear reduction of VEGF signal proximal to macrophages and subsequent attenuated neovascularization due to α-CHC injection, demonstrating that lactic acid significantly impacts macrophage function in CNV development.

In conclusion, the results presented here suggest that the glycolytic by-product lactic acid accumulates in the CNV microenvironment and contributes to neovascularization through the proangiogenic shift of infiltrated macrophages. From a therapeutic point of view, our findings imply that functional modulation of macrophages should be considered for future therapeutic applications in CNV.

Investigative Ophthalmology & Visual Science

Downloaded from iovs.arvojournals.org on 04/13/2021

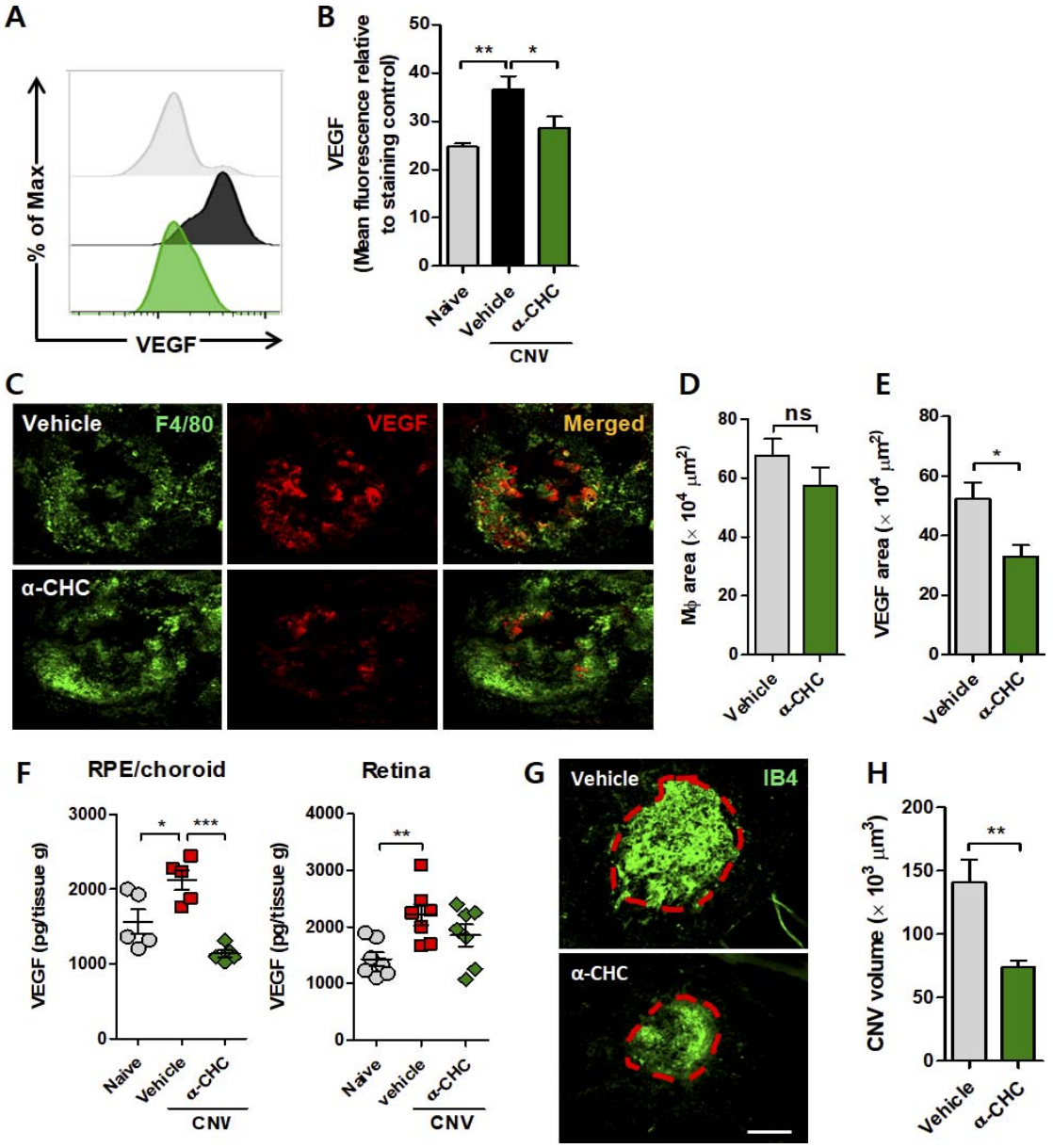

Figure 4. Blocking lactic acid uptake attenuates CNV. (**A**, **B**) Histogram (**A**) and quantitative graph (**B**) representing intracellular VEGFA staining of macrophage in CNV mice received 2 μL 3-mM α-CHC or PBS intravitreally. Data obtained by flow cytometry. $n = 6$. (**C–E**) Representative images of flat-mount choroidal tissue at 3 days after laser following PBS or 3 mM α-CHC injection were obtained by confocal immunofluorescence analysis using anti-F4/80 antibody (*green*) and anti-VEGF antibody (*red*) (**C**). *Scale bar*: 250 μm. Measurement of F4/80- (**D**) and VEGF- (**E**) stained area around the laser injury sites was performed using ImageJ software. (**F**) VEGF protein concentration in the RPE-choroid and retinal regions at 3 days after laser was quantitatively measured with the ELISA technique. (**G**, **H**) Representative confocal images of IB4-stained RPE-choroid flat-mount. Tissues were obtained at 7 days after laser shot with PBS or 2 μL 3-mM α-CHC injection. The *red dotted lines* represent the edge of IB4-stained area (**G**). Quantitative graphs representing IB4-positive volumes (**H**). *Bars* indicate means ± SEM. $^{*}P < 0.05$, $^{**}P < 0.01$, $^{***}P < 0.001$ determined by two-tailed paired *t*-test.

Acknowledgments

Supported by grants from the K-Bio Health R&D Project, Ministry of Health & Welfare, Republic of Korea (HO16C0001), the National Research Foundation of Korea (2017015015), and the Global PhD Fellowship Program of the National Research Foundation of Korea (NRF) funded by the Ministry of Education (NRF-2015H1A2A1034510). This study was also partially supported by the Brain Korea 21 PLUS Program for Creative Veterinary Science Research and Research Institute for Veterinary Science, College of Veterinary Medicine of Seoul National University.

Disclosure: **J. Song**, None; **K. Lee**, None; **S.W. Park**, None; **H. Chung**, None; **D. Jung**, None; **Y.R. Na**, None; **H. Quan**, None; **C.S. Cho**, None; **J.-H. Che**, None; **J.H. Kim**, None; **J.-H. Park**, None; **S.H. Seok**, None

References

1. Jager RD, Mieler WF, Miller JW. Age-related macular degeneration. *N Engl J Med*. 2008;358:2606–2617.
2. Ambati J, Atkinson JP, Gelfand BD. Immunology of age-related macular degeneration. *Nat Rev Immunol*. 2013;13:438–451.

Investigative Ophthalmology & Visual Science

Downloaded from iovs.arvojournals.org on 04/13/2021

3. Ambati J, Fowler BJ. Mechanisms of age-related macular degeneration. *Neuron*. 2012;75:26–39.
4. Stefansson E, Geirsdottir A, Sigurdsson H. Metabolic physiology in age related macular degeneration. *Prog Retin Eye Res*. 2011;30:72–80.
5. Osborn MP, Park Y, Parks MB, et al. Metabolome-wide association study of neovascular age-related macular degeneration. *PLoS One*. 2013;8:e72737.
6. Yokosako K, Mimura T, Funatsu H, et al. Glycolysis in patients with age-related macular degeneration. *Open Ophthalmol J*. 2014;8:39–47.
7. Orban T, Johnson WM, Dong Z, et al. Serum levels of lipid metabolites in age-related macular degeneration. *FASEB J*. 2015;29:4579–4588.
8. Lains I, Duarte D, Barros AS, et al. Human plasma metabolomics in age-related macular degeneration (AMD) using nuclear magnetic resonance spectroscopy. *PLoS One*. 2017; 12:e0177749.
9. Dietl K, Renner K, Dettmer K, et al. Lactic acid and acidification inhibit TNF secretion and glycolysis of human monocytes. *J Immunol*. 2010;184:1200–1209.
10. Draoui N, Feron O. Lactate shuttles at a glance: from physiological paradigms to anti-cancer treatments. *Dis Model Mech*. 2011;4:727–732.
11. Haas R, Smith J, Rocher-Ros V, et al. Lactate regulates metabolic and pro-inflammatory circuits in control of T cell migration and effector functions. *PLoS Biol*. 2015;13: e1002202.
12. Hirschhaeuser F, Sattler UG, Mueller-Klieser W. Lactate: a metabolic key player in cancer. *Cancer Res*. 2011;71:6921–6925.
13. Doherty JR, Cleveland JL. Targeting lactate metabolism for cancer therapeutics. *J Clin Invest*. 2013;123:3685–3692.
14. Colegio OR, Chu NQ, Szabo AL, et al. Functional polarization of tumour-associated macrophages by tumour-derived lactic acid. *Nature*. 2014;513:559–563.
15. Poitry-Yamate CL, Poitry S, Tsacopoulos M. Lactate released by Müller glial cells is metabolized by photoreceptors from mammalian retina. *J Neurosci*. 1995;15:5179–5191.
16. Adijanto J, Philp NJ. Cultured primary human fetal retinal pigment epithelium (hfRPE) as a model for evaluating RPE metabolism. *Exp Eye Res*. 2014;126:77–84.
17. Hurley JB, Lindsay KJ, Du J. Glucose, lactate, and shuttling of metabolites in vertebrate retinas. *J Neurosci Res*. 2015;93: 1079–1092.
18. Kinnunen K, Petrovski G, Moe MC, Berta A, Kaarniranta K. Molecular mechanisms of retinal pigment epithelium damage and development of age-related macular degeneration. *Acta Ophthalmol*. 2012;90:299–309.
19. Gallagher-Colombo S, Maminishkis A, Tate S, Grunwald GB, Philp NJ. Modulation of MCT3 expression during wound healing of the retinal pigment epithelium. *Invest Ophthalmol Vis Sci*. 2010;51:5343–5350.
20. Kruger NJ, Troncoso-Ponce MA, Ratcliffe RG. 1H NMR metabolite fingerprinting and metabolomic analysis of perchloric acid extracts from plant tissues. *Nat Protoc*. 2008;3:1001–1012.
21. Yi X, Ogata N, Komada M, et al. Vascular endothelial growth factor expression in choroidal neovascularization in rats. *Graefes Arch Clin Exp Ophthalmol*. 1997;235:313–319.
22. Winkler BS. *A Quantitative Assessment of Glucose Metabolism in the Isolated Retina*. Amsterdam, The Netherlands: Elsevier; 1995.
23. Zhu D, Zhou J, Xu X. Influence of lactic acid on differential expression of vascular endothelial growth factor and pigment epithelium-derived factor in explants of rat retina. *Curr Eye Res*. 2012;37:1025–1029.
24. Hermansen L, Stensvold I. Production and removal of lactate during exercise in man. *Acta Physiol Scand*. 1972;86:191–201.
25. Winkler BS, Starnes CA, Sauer MW, Firouzgan Z, Chen SC. Cultured retinal neuronal cells and Müller cells both show net production of lactate. *Neurochem Int*. 2004;45:311–320.
26. Murakami N, Yokomizo T, Okuno T, Shimizu T. G2A is a proton-sensing G-protein-coupled receptor antagonized by lysophosphatidylcholine. *J Biol Chem*. 2004;279:42484–42491.
27. Kabarowski JH. G2A and LPC: regulatory functions in immunity. *Prostaglandins Other Lipid Mediat*. 2009;89:73–81.
28. Bolick DT, Skaflen MD, Johnson LE, et al. G2A deficiency in mice promotes macrophage activation and atherosclerosis. *Circ Res*. 2009;104:318–327.
29. Chen P, Zuo H, Xiong H, et al. Gpr132 sensing of lactate mediates tumor-macrophage interplay to promote breast cancer metastasis. *Proc Natl Acad Sci U S A*. 2017;114:580–585.
30. Tsutsumi C, Sonoda KH, Egashira K, et al. The critical role of ocular-infiltrating macrophages in the development of choroidal neovascularization. *J Leukoc Biol*. 2003;74:25–32.
31. Krause TA, Alex AF, Engel DR, Kurts C, Eter N. VEGF-production by CCR2-dependent macrophages contributes to laser-induced choroidal neovascularization. *PLoS One*. 2014; 9:e94313.
32. Xie P, Kamei M, Suzuki M, et al. Suppression and regression of choroidal neovascularization in mice by a novel CCR2 antagonist, INCB3344. *PLoS One*. 2011;6:e28933.
33. Kim SJ, Lee HJ, Yun JH, Ko JH, Choi DY, Oh JY. Intravitreal TSG-6 suppresses laser-induced choroidal neovascularization by inhibiting CCR2+ monocyte recruitment. *Sci Rep*. 2015;5: 11872.
34. Espinosa-Heidmann DG, Suner IJ, Hernandez EP, Monroy D, Csaky KG, Cousins SW. Macrophage depletion diminishes lesion size and severity in experimental choroidal neovascularization. *Invest Ophthalmol Vis Sci*. 2003;44:3586–3592.
35. Sakurai E, Anand A, Ambati BK, van Rooijen N, Ambati J. Macrophage depletion inhibits experimental choroidal neovascularization. *Invest Ophthalmol Vis Sci*. 2003;44:3578–3585.
36. Gragoudas ES, Adamis AP, Cunningham ET Jr, Feinsod M, Guyer DR; VEGF Inhibition Study in Ocular Neovascularization Clinical Trial Group. Pegaptanib for neovascular age-related macular degeneration. *N Engl J Med*. 2004;351:2805–2816.
37. Rosenfeld PJ, Brown DM, Heier JS, et al. Ranibizumab for neovascular age-related macular degeneration. *N Engl J Med*. 2006;355:1419–1431.
38. Enslow R, Bhuvanagiri S, Vegunta S, Cutler B, Neff M, Stagg B. Association of anti-VEGF injections with progression of geographic atrophy. *Ophthalmol Eye Dis*. 2016;8:31–32.
39. He L, Marneros AG. Doxycycline inhibits polarization of macrophages to the proangiogenic M2-type and subsequent neovascularization. *J Biol Chem*. 2014;289:8019–8028.
40. Zandi S, Nakao S, Chun KH, et al. ROCK-isoform-specific polarization of macrophages associated with age-related macular degeneration. *Cell Rep*. 2015;10:1173–1186.
41. Sonveaux P, Copetti T, De Saedeleer CJ, et al. Targeting the lactate transporter MCT1 in endothelial cells inhibits lactate-induced HIF-1 activation and tumor angiogenesis. *PLoS One*. 2012;7:e33418.
42. Ruan GX, Kazlauskas A. Lactate engages receptor tyrosine kinases Axl, Tie2, and vascular endothelial growth factor receptor 2 to activate phosphoinositide 3-kinase/Akt and promote angiogenesis. *J Biol Chem*. 2013;288:21161–21172.

Investigative Ophthalmology & Visual Science

Downloaded from iovs.arvojournals.org on 04/13/2021